[1]Institute of Physics of the University of São Paulo &
[2]The George Washington University

Extensions of Chiral Perturbation Theory for the Analysis of LatticeQCD data

R. Molina[1]
M. Döring, M. Mai, B. Hu, D. Guo, A. Alexandru

February 13, 2018

Content

Methods

Based on general properties of the scattering amplitudes such as Analyticity, Unitarity, Crossing symmetry, applied often in combination with EFT (chiral symmetry (if not, can be added as a constraint))

- Unitarized Chiral Perturbation Theory. Oller, Oset, Pelaez (1997)
- Inverse Amplitude Method. Truon, Herrero, Dobado, Pelaez (1988)
- Roy-Steiner equations based on dispersion relations. Roy, Steiner, Hite (1971)
- N/D method, Oller (1998)
- Bethe-Salpeter ...

Lattice data + EFT (chiral symmetry) + general properties of the scattering amplitudes can be a powerful tool !!

Chiral Perturbation Theory

- ChPT expansion of the amplitude for meson-meson scattering

$$t(s) = t_2(s) + t_4(s) + ...t_{2k} = \mathcal{O}(p^{2k}) \tag{1}$$

- Lowest-order Chiral Lagrangian

$$\mathcal{L}_2 = \frac{f^2}{4}\langle \partial_\mu U^\dagger \partial^\mu U + M(U + U^\dagger)\rangle \tag{2}$$

$$\begin{aligned}
\mathcal{L}_4 = \quad & L_1\langle \partial_\mu U^\dagger \partial^\mu U\rangle^2 + L_2\langle \partial_\mu U^\dagger \partial_\nu U\rangle\langle \partial^\mu U^\dagger \partial^\nu U\rangle \\
& + L_3\langle \partial_\mu U^\dagger \partial^\mu U \partial_\nu U^\dagger \partial^\nu U\rangle + L_4\langle \partial U^\dagger \partial^\mu U\rangle\langle U^\dagger M + M^\dagger U\rangle \\
& + L_5\langle \partial_\mu U^\dagger \partial^\mu U(U^\dagger M + M^\dagger U)\rangle + L_6\langle U^\dagger M + M^\dagger U\rangle^2 \\
& + L_7\langle U^\dagger M - M^\dagger U\rangle^2 + L_8\langle M^\dagger U M^\dagger U + U^\dagger M U^\dagger M\rangle
\end{aligned} \tag{3}$$

Chiral Perturbation Theory

where $U(\phi) = \exp(i\sqrt{2}\Phi/f)$, and

$$\Phi(x) = \begin{pmatrix} \frac{\pi^0}{\sqrt{2}} + \frac{\eta}{\sqrt{6}} & \pi^+ & K^+ \\ \pi^- & -\frac{\pi^0}{\sqrt{2}} + \frac{\eta}{\sqrt{6}} & K^0 \\ K^- & \bar{K}^0 & -\frac{2}{\sqrt{6}}\eta \end{pmatrix}_\mu \quad (4)$$

$$M = \begin{pmatrix} m_\pi^2 & 0 & 0 \\ 0 & m_\pi^2 & 0 \\ 0 & 0 & 2m_K^2 - m_\pi^2 \end{pmatrix} \quad (5)$$

[1] J. Gasser and H. Leutwyler, Annals Phys. **158**, 142 (1984)

[2] J. Gasser and H. Leutwyler, Nucl. Phys. B **250**, 465 (1985)

[3] J. A. Oller, E. Oset and J. R. Pelaez, Phys. Rev. D **59**, 074001 (1999)

Unitary amplitude in coupled channels

- **Unitarity in coupled channels:**

$$\boxed{\mathrm{Im}\, T_{if} = T_{in} \sigma_{nn} T^*_{nf}} \qquad (6)$$

with $\sigma_{nn}(s) = -\frac{k_n}{8\pi\sqrt{s}}\theta(s - (m_{1n} + m_{2n})^2)$ and k_n is the on-shell c.m. momentum of the intermediate meson.

K-matrix formalism: $T^{-1} = K^{-1} - i\sigma$, where $K^{-1} = \mathrm{Re}\, T^{-1}$. And,

$$\sigma = T^{-1}\mathrm{Im}\, T T^{*-1} = \frac{1}{2i} T^{-1}(T - T^*) T^{*-1} = \frac{1}{2i}(T^{-1*} - T^{-1}) = -\mathrm{Im}\, T^{-1}.$$

Therefore, $T^{-1} = \mathrm{Re}\, T^{-1} + i\mathrm{Im}\, T^{-1} = \mathrm{Re}\, T^{-1} - i\sigma$, or

$$\boxed{T = [\mathrm{Re}\, T^{-1} - i\sigma]^{-1}} \qquad (7)$$

Unitarity amplitude in coupled channels

Expansion of T^{-1} in powers of p^2:

$$T \simeq T_2 + T_4 + ...$$
$$T^{-1} \simeq T_2^{-1}[1 + T_4 T_2^{-1} + ...]^{-1} \simeq T_2^{-1}[1 - T_4 T_2^{-1} ...]$$
$$T = T_2 T_2^{-1}[\mathrm{Re}\, T^{-1} - i\sigma]^{-1} T_2^{-1} T_2 = T_2[T_2 \mathrm{Re}\, T^{-1} T_2 - i T_2 \sigma T_2]^{-1} T_2$$

Inserting the expansion of T^{-1} in the first member of [],

$T_2 = \mathrm{Re}\, T_2$, $\mathrm{Im}\, T = \mathrm{Im}\, T_4 = T_2 \sigma T_2$.

$T_2 \mathrm{Re}\, T^{-1} T_2 = T_2 \mathrm{Re}(T_2^{-1}(1 - T_4 T_2^{-1}))T_2 = T_2 - \mathrm{Re}\, T_4$.

Thus,

$$T = T_2[T_2 - \mathrm{Re}\, T_4 - i \mathrm{Im}\, T_4]^{-1} T_2 \longrightarrow T = T_2[T_2 - T_4]^{-1} T_2 \qquad (8)$$

$\mathrm{Re}\, T_4 \simeq T_4^p + T_2 \mathrm{Re} G T_2$, $\mathrm{Im}\, G = \sigma$, $G \equiv$ Two meson func. loop,

$$\boxed{T = T_2[T_2 - T_4^p - T_2 G T_2]^{-1} T_2} \qquad (9)$$

UChPT (NLO) Oller, Oset, Pelaez (1999)

$V_{\rm IAM}$ is the kernel of the scattering equation:

$$T = T + VGT \longrightarrow T = [I - V_{\rm IAM} G]^{-1} V_{\rm IAM}, \quad \text{with} \qquad (10)$$

$$\boxed{V_{\rm IAM} = [1 - V_4 (V_2)^{-1}]^{-1} V_2} \qquad (11)$$

$$V_2 = \frac{m_\pi^2 - s}{f_\pi^2}$$

$$\begin{aligned} V_4 = &-\frac{4}{f^4}((2\,L_1 + L_3)(s - 2\,m_\pi^2)^2 \\ &+ L_2((t - 2\,m_\pi^2)^2 + (u - 2\,m_\pi^2)^2) \\ &+ 2(2\,L_4 + L_5) m_\pi^2 (s - 2\,m_\pi^2) \\ &+ 4(2\,L_6 + L_8) m_\pi^4) \end{aligned}$$

$I = L = 1$:

$$\longrightarrow \boxed{V_{\pi\pi}^{11} = -2p^2/(3(f_\pi^2 - 8\hat{l}_1\, m_\pi^2 + 4\hat{l}_2\, E^2))} \qquad (12)$$

and, $\hat{l}_1 = 2\,L_4 + L_5, \quad \hat{l}_2 = 2\,L_1 - L_2 + L_3.$

UChPT

$$V^{00}_{\pi\pi}(s) = \frac{3(m_\pi^2 - 2s)^2}{6f_\pi^2(m_\pi^2 - 2s) + 8(L_a m_\pi^4 + s(L_b m_\pi^2 + L_c s))}$$

$$\begin{aligned} L_a &= -36\hat{l}_1 + 44\hat{l}_2 + 20(5L_2 + 6L_6 + 3L_8)\,, \\ L_b &= 12\hat{l}_1 - 40\hat{l}_2 - 80L_2\,, \\ L_c &= 11\hat{l}_2 + 25L_2\,, \end{aligned} \tag{13}$$

Sets of LECs used here,

- ρ: $\hat{l}_1$, $\hat{l}_2$
- σ: L_a, L_b, L_c
- $\sigma + \rho$: $\hat{l}_1$, $\hat{l}_2$, L_2 and L_8.
- $L_6 = 0$

Second Riemann Sheet

Schwartz reflexion theorem: $f(z)$ is analytic in a region of the complex plane in which f is real, then

$$f(z^*)^* = f(z) \tag{14}$$

For the loop function, above threshold, $\text{Re}\sqrt{s} > m + M$,

$$G(\sqrt{s} - i\epsilon) = (G(\sqrt{s} + i\epsilon))^* = G(\sqrt{s} + i\epsilon) - i\,2\mathrm{Im}\,G(\sqrt{s} + i\epsilon) \tag{15}$$

Since the beginning of R2 is equal to the end of R1,

$$G^{II}(\sqrt{s} + i\epsilon) = G^{I}(\sqrt{s} - i\epsilon) = G^{I}(\sqrt{s}) + i\epsilon) - i\,2\mathrm{Im}\,G^{I}(\sqrt{s} + i\epsilon) \tag{16}$$

Since $\mathrm{Im}\,G^{I}(\sqrt{s} + i\,\epsilon) = -\frac{q}{8\,\pi\sqrt{s}}$,

$$\boxed{G^{II}(\sqrt{s}) = G^{I}(\sqrt{s}) + i\,\frac{q}{4\pi\sqrt{s}}, \quad \mathrm{Im}\,q > 0} \tag{17}$$

Meson decay constants from SU(3) UCh PT extrapolation

The physical masses can be expressed as a function the leading order masses (M_0), LEC's (L^r) and pseudoscalar decay constants (f).

$$M_\pi^2 = M_{0\,\pi}^2 \left[1 + \mu_\pi - \frac{\mu_\eta}{3} + \frac{16 M_{0\,K}^2}{f_0^2}\left(2L_6^r - L_4^r\right) + \frac{8 M_{0\,\pi}^2}{f_0^2}\left(2L_6^r + 2L_8^r - L_4^r - L_5^r\right)\right]$$

$$M_K^2 = M_{0\,K}^2 \left[1 + \frac{2\mu_\eta}{3} + \frac{8 M_{0\,\pi}^2}{f_0^2}\left(2L_6^r - L_4^r\right) + \frac{8 M_{0\,K}^2}{f_0^2}\left(4L_6^r + 2L_8^r - 2L_4^r - L_5^r\right)\right],$$

$$M_\eta^2 = M_{0\,\eta}^2 \left[1 + 2\mu_K - \frac{4}{3}\mu_\eta + \frac{8 M_{0\,\eta}^2}{f_0^2}(2L_8^r - L_5^r) + \frac{8}{f_0^2}(2M_{0\,K}^2 + M_{0\,\pi}^2)(2L_6^r - L_4^r)\right]$$

$$+ M_{0\,\pi}^2 \left[-\mu_\pi + \frac{2}{3}\mu_K + \frac{1}{3}\mu_\eta\right] + \frac{128}{9 f_0^2}(M_{0\,K}^2 - M_{0\,\pi}^2)^2 (3L_7 + L_8^r),$$

$$\mu_P = \frac{M_{0\,P}^2}{32\pi^2 f_0^2} \log \frac{M_{0\,P}^2}{\mu^2}, \qquad P = \pi, K, \eta\ ,$$

where f_0 is the pion decay constant in the chiral limit, $4\pi f_0 \simeq 1.2$ GeV, μ is the regularization scale.

Meson decay constants from SU(3) UCh PT extrapolation

One loop SU(3) UChPT,

$$f_\pi = f_0 \left[1 - 2\mu_\pi - \mu_K + \frac{4M_{0\,\pi}^2}{f_0^2} \left(L_4^r + L_5^r \right) + \frac{8M_{0\,K}^2}{f_0^2} L_4^r \right] , \tag{18}$$

$$f_K = f_0 \left[1 - \frac{3\mu_\pi}{4} - \frac{3\mu_K}{2} - \frac{3\mu_\eta}{4} + \frac{4M_{0\,\pi}^2}{f_0^2} L_4^r + \frac{4M_{0\,K}^2}{f_0^2} \left(2L_4^r + L_5^r \right) \right] , \tag{19}$$

$$f_\eta = f_0 \left[1 - 3\mu_K + \frac{4L_4^r}{f_0^2} \left(M_{0\,\pi}^2 + 2M_{0\,K}^2 \right) + \frac{4M_{0\,\eta}^2}{f_0^2} L_5^r \right] . \tag{20}$$

[1] J. Nebreda and J. R. Pelaez., Phys. Rev. D **81**, 054035 (2010)

Formalism in the finite volume

Two-meson-loop function G:

$$G = G^{co}(E) = \int_{q<q_{max}} \frac{d^3q}{(2\pi)^3} \frac{\omega_1 + \omega_2}{2\omega_1\omega_2} \frac{2M_i}{E^2 - (\omega_1+\omega_2)^2 + i\epsilon} \qquad (21)$$

where $\omega_i = \sqrt{m_i^2 + |\vec{q}_i\,|^2}$ is the energy and $\vec{q}$ stands for the momentum of the meson in the channel i. In the finite volume, the momenta is quantized,

$$\vec{q}_i = \frac{2\pi}{L}\vec{n}_i; \qquad T \longrightarrow \tilde{T}; \qquad G(E) \longrightarrow \tilde{G}(E)\ , \qquad (22)$$

[1] M. Doring, U. G. Meißner, E. Oset and A. Rusetsky, Eur. Phys. J. A47, 139 (2011)

[2] M. Doring, J. Haidenbauer, U. G. Meißner, and A. Rusetsky, Eur. Phys. J. A47, 163 (2011)

Formalism in the finite volume

where

$$\tilde{G}(E) = \frac{1}{L^3} \sum_{\vec{q}_i} I(E, \vec{q}_i) \,, \tag{23}$$

with

$$I(E, \vec{q}_i) = \frac{\omega_1(\vec{q}_i) + \omega_2(\vec{q}_i)}{2\omega_1(\vec{q}_i)\omega_2(\vec{q}_i)} \frac{1}{(E)^2 - (\omega_1(\vec{q}_i) + \omega_2(\vec{q}_i))^2} \tag{24}$$

and $\vec{q} = \frac{2\pi}{L}(n_x, n_y, n_z)$. The formalism can also be made independent of q_{max} and related to α.

$$\tilde{G} = G^{DR} + \lim_{q_{max}\to\infty} \left(\frac{1}{L^3} \sum_{q<q_{max}} I(E, \vec{q}) - \int_{q<q_{max}} \frac{d^3q}{(2\pi^3)} I(E, \vec{q}) \right)$$

$$\equiv G^{DR} + \lim_{q_{max}\to\infty} \delta G \,, \tag{25}$$

[1] A. Martinez Torres, L. R. Dai, C. Koren, D. Jido and E. Oset, Phys. Rev. D **85**, 014027 (2012)

Formalism in the finite volume

- Bethe-Salpeter equation in finite volume,

$$\tilde{T}^{-1} = V^{-1} - \tilde{G} \tag{26}$$

- Energy levels in the box in the presence of interaction V correspond to the condition

$$\boxed{\det(I - V\tilde{G}) = 0} \tag{27}$$

- One-channel-amplitude in infinite volume T

$$T = (\tilde{G}(E_i) - G(E_i))^{-1}. \tag{28}$$

- Phase shift:

$$\boxed{\tan\delta = -k/(8\pi E \Delta G)} \tag{29}$$

Boost, Asymmetric Boxes and Partial Wave Decomposition

Doering, Meißner, Oset, Rusetsky (2012)

$\vec{q}_1, \vec{q}_2 = \vec{P} - \vec{q}_1$, $s \equiv W^2 = (P^0)^2 - \vec{P}^2$, and $\vec{q}^*$ the momenta in the CM frame

$$\int \frac{d^3\vec{q}^{\,*}}{(2\pi)^3} I(|\vec{q}^{\,*}|) \to \tilde{G}(P) = \frac{1}{\eta L^3} \frac{\sqrt{s}}{P^0} \sum_{\vec{n}} I(|\vec{q}^{\,*}(\vec{q})|). \qquad (30)$$

$$\vec{q}^{\,*}_{1,2} = \vec{q}_{1,2} + \left[\left(\frac{\sqrt{s}}{P^0} - 1 \right) \frac{\vec{q}_{1,2} \cdot \vec{P}}{|\vec{P}|^2} - \frac{q^{*0}_{1,2}}{P^0} \right] \vec{P}; \text{ with } \vec{q} = \frac{2\pi}{L}(n_x, n_y, \frac{n_z}{\eta}), \vec{P} = \frac{2\pi}{L}(N_x, N_y, \frac{N_z}{\eta}).$$

$$\tilde{T}_{lm,l'm'}(p,p') = V_l(p,p')\delta_{ll'}\delta_{mm'} + \sum_{l''m''} V_l(p, q^{\mathrm{on},*}) \tilde{G}_{lm,l''m''}(q^{\mathrm{on},*}) \tilde{T}_{l''m'',lm}(q^{\mathrm{on},*}, p')$$

$$\boxed{\det(\delta_{ll'}\delta_{mm'} - V_l(q^{\mathrm{on},*}, q^{\mathrm{on},*}) \tilde{G}_{lm,l'm'}(q^{\mathrm{on},*})) = 0} \qquad (32)$$

Irreducible representations for asymmetric boxes and boost $\vec{P} = \frac{2\pi}{\eta L}(0,0,1)$,

$$\mathrm{I} = \mathrm{L} = 0 \longrightarrow \mathrm{A}^+ : -1 + \mathrm{V}_0 \mathrm{G}_{00,00} = 0$$

$$\mathrm{I} = \mathrm{L} = 1 \longrightarrow \mathrm{A}_2^- : -1 + \mathrm{V}_1 \mathrm{G}_{10,10} = 0; \mathrm{E}^- : -1 + \mathrm{V}_1 \mathrm{G}_{11,11} = 0$$

The σ resonance

Anlyses

$m_\pi = 227, 315$ MeV

Conformal mapping:

- cm1: σ, individual
- cm2: σ, individual

Chiral unitary approach:

- chm1: σ, combined
- chm2: $\sigma + \rho$, individual and combined

Conformal mapping

Parameterization

- Most general form of the K-matrix as an analytical function of energy
- The convergence of the series is improved by mapping it onto the interior of a disk

$$\omega^{[\mathrm{cm1}]}(s) = \frac{\sqrt{s} - \alpha\sqrt{4m_K^2 - s}}{\sqrt{s} + \alpha\sqrt{4m_K^2 - s}}, \tag{33}$$

$$\omega^{[\mathrm{cm2}]}(s) = \frac{\sqrt{s} - \alpha}{\sqrt{s} + \alpha}, \tag{34}$$

with $\alpha = 1$; $m_K = 550\,\mathrm{MeV}$ [cm1] and $\alpha = 1000$ MeV [cm2].

I. Caprini. Phys. Rev. D77 (2008)

Conformal mapping

***K* matrix**:

$$K_{00}^{-1}(s) = \frac{1}{16\pi} \frac{M_\pi^2}{s_A - s} \left(\frac{2s_A}{M_\pi \sqrt{s}} + B_0 + B_1 \omega(s) + ... \right) \qquad (35)$$

Chiral symmetry dictates that $T_{00}(s)$ must vanish for $s = s_A \sim M_\pi^2/2$.

- α is fixed (not significant improved if running).
- Two fitting parameters, B_0 and B_1.

Scattering amplitude in the finite volume and $I = L = 0$ channel,

$$\tilde{T}_{00}(s) = \frac{1}{K_{00}^{-1}(s) - \tilde{G}(s)} , \qquad (36)$$

Solution: Energies E_0^i with covariance matrix C,

$$\chi^2 = (E - E_0)^T \cdot C^{-1} \cdot (E - E_0) \qquad (37)$$

which provide a minimal χ^2.

Results: Conformal mapping

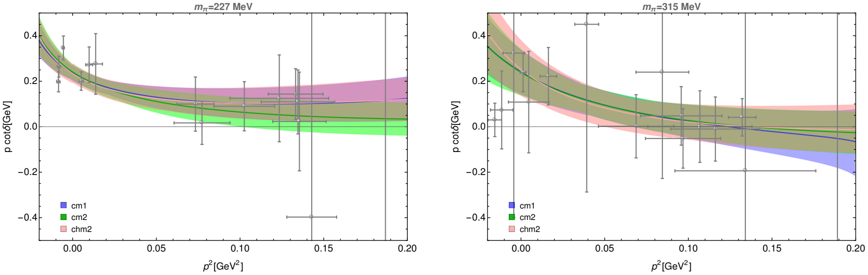

Figure: $p\cot\delta$ as a function of p^2 in the conformal parameterizations for the $I = L = 0$ channel, [cm1] and [cm2], in comparison with the individual $\sigma + \rho$ chiral fits.

Pole positions

Conformal mapping vs. UChPT fits

Par.	Fitted data set	$M_\pi = 227$ MeV			$M_\pi = 315$ MeV		
		Rez_0	- Imz_0	g	Rez_0	- Imz_0	g
cm1	σ_{227}	460^{+30}_{-60}	180^{+30}_{-30}	$3.2^{+0.1}_{-0.1}$	–	–	–
	σ_{315}	–	–	–	660^{+50}_{-70}	150^{+40}_{-50}	$4.0^{+0.2}_{-0.2}$
cm2	σ_{227}	475^{+30}_{-60}	176^{+50}_{-40}	$3.3^{+0.3}_{-0.2}$	–	–	–
	σ_{315}	–	–	–	660^{+50}_{-90}	140^{+40}_{-50}	$3.9^{+0.2}_{-0.2}$
chm2	σ_{227} ρ_{227}	460^{+30}_{-40}	160^{+30}_{-30}	$3.0^{+0.1}_{-0.1}$	–	–	–
	σ_{315} ρ_{315}	–	–	–	660^{+40}_{-60}	120^{+40}_{-40}	$3.6^{+0.1}_{-0.1}$

Table: Pole positions (z_0 in MeV) and corresponding couplings to $\pi\pi$ channel (g in GeV) in the conformal mapping parameterizations, [cm1] and [cm2], and in the UChPT individual fits [chm2].

Combined fits from UChPT

σ [chm1] and $\sigma + \rho$ [chm2] fits

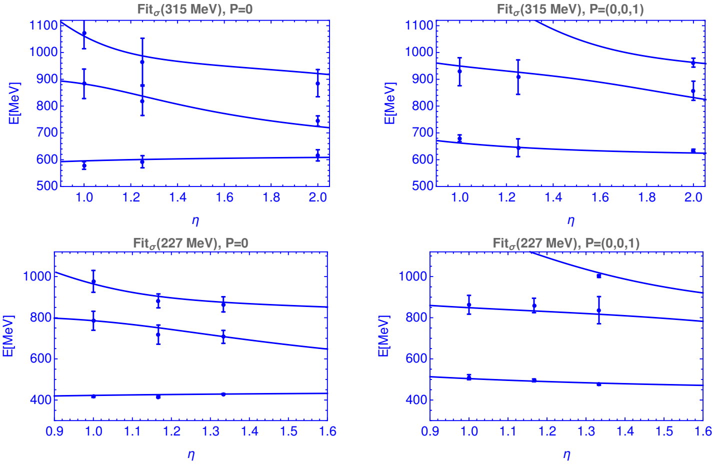

Figure: Energy levels in the σ fits [chm1] to $m_\pi = 227, 315$ MeV energy levels. The energy levels are similar when the ρ meson is included [chm2].

Combined fits from UChPT

σ [chm1] and $\sigma + \rho$ [chm2] fits

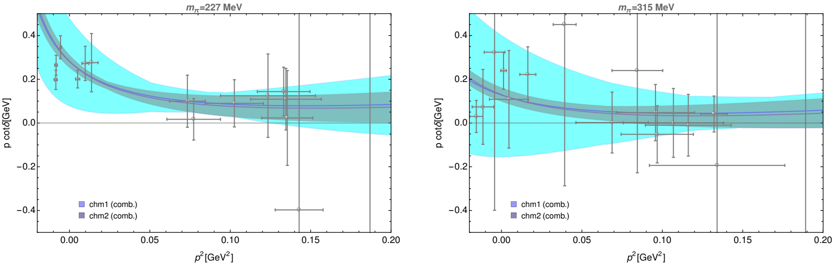

Figure: $p\cot\delta$ in the chiral combined fits for two pion masses, in the $\mathrm{I}=\mathrm{L}=0$ channel, and $\mathrm{I}=\mathrm{L}=0$ and $\mathrm{I}=\mathrm{L}=1$ channels.

Extrapolation to the physical point

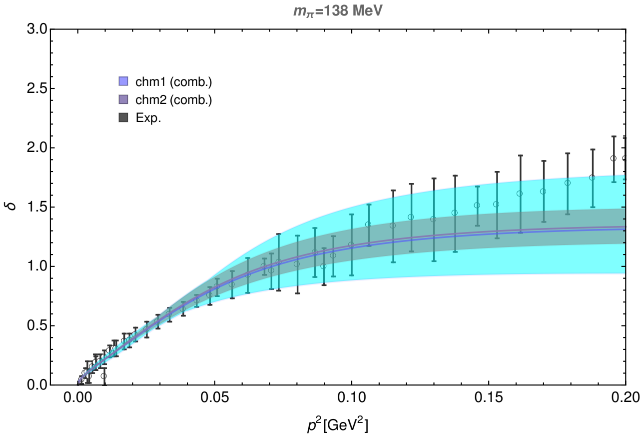

Figure: Comparison to the experimental data of Batley, 2010; Frogatt,1977; Estabrooks,1974; Hyams,1973; Protopopescu,1973; Grayer,1974.

Pion mass dependence

Pole position z_0

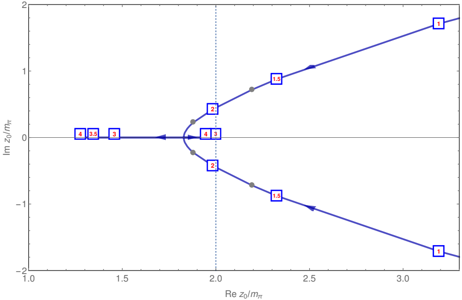

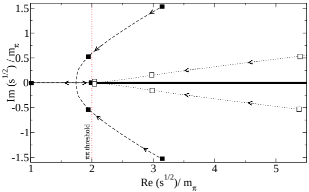

Figure: Pole position z_0 in units of m_π. In the boxes, the pion mass in terms of the physical one, $m_{\pi,0} = 138$ MeV. Gray dots are the masses studied here (lattice data).

IAM solution (exp. data). Hanhart, Pelaez, Rios (2014)

In both cases it becomes bound at 3 $m_{\pi,0}$

Pion mass dependence

Coupling g_π

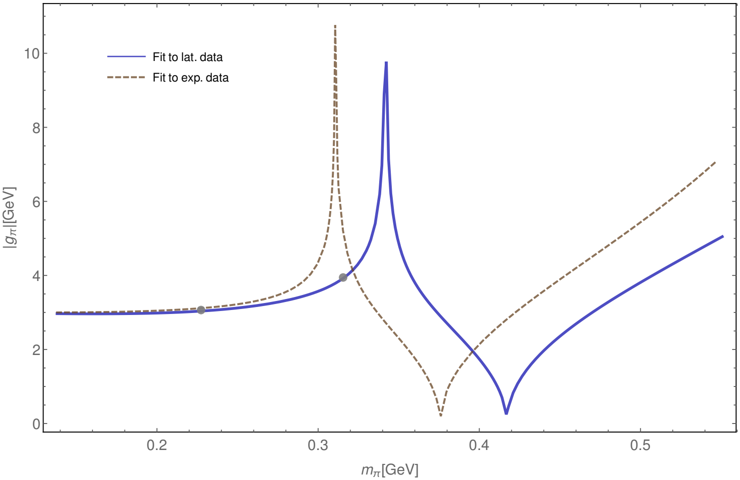

Figure: Coupling g_π as a function of m_π. In gray the masses studied here.

UChPT vs. other works (σ)

Par.	M_π = 138 MeV			M_π = 227 MeV			M_π = 315 MeV		
Fitted data set	Rez_0	- Imz_0	g	Rez_0	- Imz_0	g	Rez_0	- Imz_0	g
chm1 $\sigma_{227,315}$	440^{+60}_{-90}	240^{+20}_{-50}	$3.0^{+0.2}_{-0.6}$	490^{+100}_{-70}	170^{+40}_{-110}	$3.0^{+0.7}_{-0.5}$	590^{+130}_{-120}	80^{+150}_{-80}	$4.0^{+4.0}_{-2.0}$
chm2 $\sigma_{227,315}$ $\rho_{227,315}$	440^{+10}_{-16}	240^{+20}_{-20}	$3.0^{+0.0}_{-0.0}$	500^{+20}_{-20}	160^{+15}_{-15}	$3.0^{+0.0}_{-0.1}$	600^{+30}_{-40}	80^{+20}_{-80}	$3.9^{+5.0}_{-0.2}$
Par.	M_π = 138 MeV			M_π = 236 MeV			M_π = 391 MeV		
Fitted data set	Rez_0	- Imz_0	g	Rez_0	- Imz_0	g	Rez_0	- Imz_0	g
Pelaez, 2015 Exp.	449^{+22}_{-16}	275^{+12}_{-12}	$3.5^{+0.3}_{-0.2}$	-	-	-	-	-	-
Doring, Mai 2016 $(\sigma/\rho)_{236,391}$	452^{+1}_{-0}	144^{+0}_{-4}	$2.6^{+0.0}_{-0.0}$	515^{+0}_{-0}	104^{+3}_{-0}	$3.0^{+0.0}_{-0.0}$	771^{+1}_{-0}	0	$3.0^{+0.0}_{-0.1}$
Briceño, Wilson 2016 $\sigma_{236,391}$	-	-	-	667^{+113}_{-113}	201^{+84}_{-84}	$2.9^{+0.7}_{-0.7}$	753^{+8}_{-8}	0	$2.3^{+0.3}_{-0.3}$
chm2 $\sigma_{227,315}$ $\rho_{227,315}$	440^{+10}_{-16}	240^{+20}_{-20}	$3.0^{+0.0}_{-0.0}$	510^{+20}_{-20}	160^{+15}_{-15}	$3.1^{+0.0}_{-0.1}$	781^{+2}_{-20}	$0.0^{+0.0}_{-0.0}$	$2.1^{+2.6}_{-2.0}$

Table: Pole positions (z_0 in MeV) and corresponding couplings to $\pi\pi$ channel (g in GeV) in the chiral unitary approach [chm1] and [chm2].

UChPT vs. other works (σ)

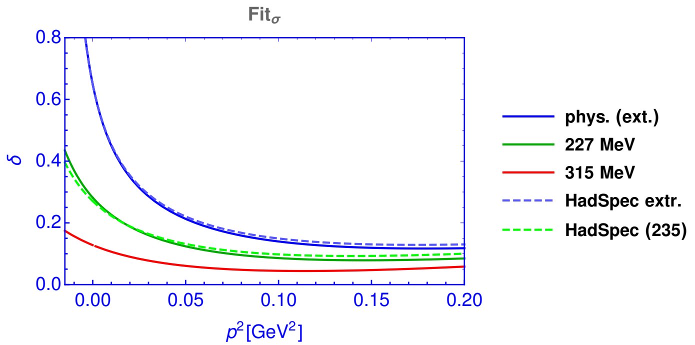

Figure: $p\cot\delta$ in comparison with the result of Bricenõ, Wilson (2016) and the analysis of Döring, Mai (2016)

The ρ meson

Analyses

- GWU $N_f = 2$ energy levels (comparison to other $N_f = 2$ lattice data)
- Other $N_f = 2$ lattice data
- $N_f = 2 + 1$ lattice data

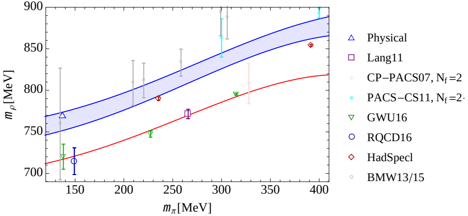

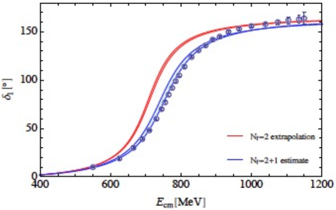

m_π [MeV]	$\hat{l}_1 \times 10^3$	$\hat{l}_2 \times 10^3$	m_ρ [MeV]	Γ_ρ [MeV]
315	1.5(5)	−3.7(2)	796(1)	35(1)
138			704(5)	110(3)
226	2(1)	−3.5(2)	748(1)	77(1)
138			719(4)	120(3)
226, 315	2.26(14)	−3.44(3)		
138			720(1)	121(1)

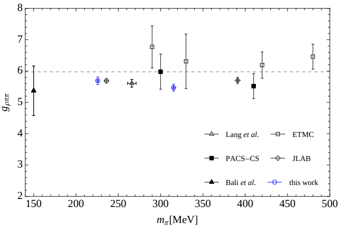

$N_f = 2$ GWU data
Comparison to other data

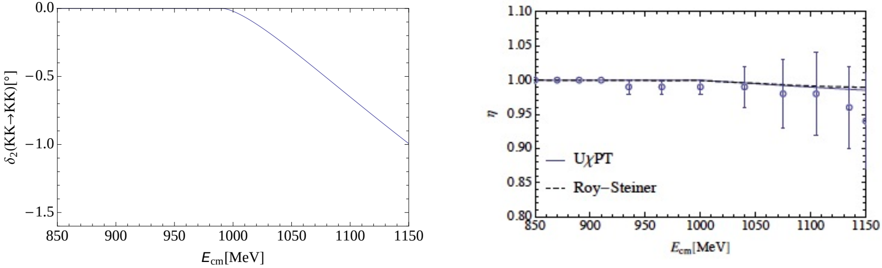

Figure: Left: The $K\bar{K}$ phase shift (physical pion masses) is small and negative. Same sign than in the work of Wilson et al. (2015). Right: Comparison of the inelasticity from UChPT with the experiment and the Roy-Steiner solution.

Analysis of $N_f = 2$ lattice data: RQCD, GWU, QCDSF, Lang, ETMC and CP-PACS

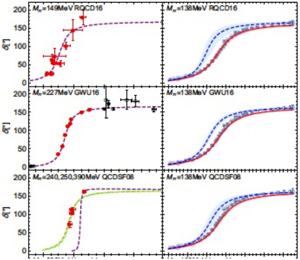

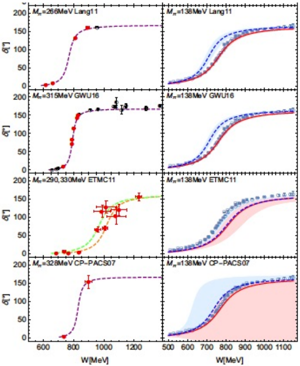

$K\bar{K}$ channel included a posteriori (red)

B. H, R. Molina, M. Döring and A. Alexandru, Phys. Rev. Let. 117 (2016)

D. Guo, A. Alexandru, R. Molina and M. Döring, Phys. Rev. D94 (2016)

[1] G. S. Bali et al . [RQCD Collaboration], Phys. Rev. D93 (2016)

[2] M. Göckeler et al. [QCDSF Collaboration], PoS LATTICE (2008)

[3] C. B. Lang, D. Mohler, S. Prelovsek and M. Vidmar, Phys. Rev. D. 83 (2011)

[4] X. Feng, K. Jansen and D. B. Renner [ETMC Collaboration], Phys. Rev. D83 (2011)

[5] S. Aoki et al. [CP-PACS Collaboration], Phys. Rev. D76 (2007)

Analysis of $N_f = 2$ lattice data: RQCD, GWU, QCDSF, Lang, ETMC and CP-PACS

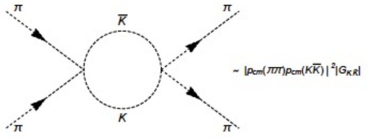

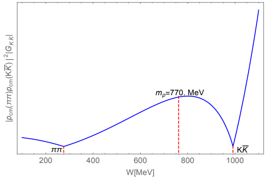

Ratio of the couplings of the ρ meson to $\pi\pi$ and $K\bar{K}$		
	Oller/Pelaez(1999)	Guo/Oller(2012)
$\frac{g_{K\bar{K}}}{g_{\pi\pi}}$	0.54	0.64

Not that small!! NLO UChPT vs. One-loop UChPT

Analysis of $N_f = 2$ lattice data: RQCD, GWU, QCDSF, Lang, ETMC and CP-PACS

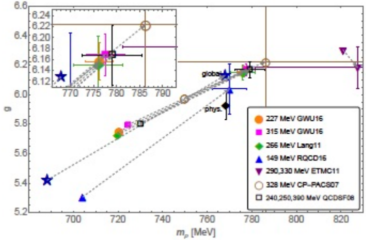

Figure: Effect of the $K\bar{K}$ channel in the (m_ρ, g) plane indicated with arrows, after chiral extrapolation to the physical pion mass.

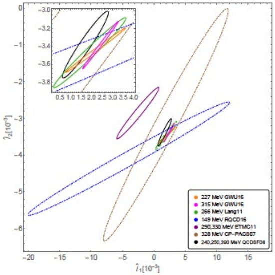

Figure: Error ellipses in the $(\hat{l}_1, \hat{l}_2)$ plane.

Most ellipses in the $(\hat{l}_1, \hat{l}_2)$ plane from the $N_f = 2$ lattice data analysis have a common overlap area.

$N_f = 2 + 1$ lattice data analysis

[1] D. J. Wilson, R. A. Briceño, J. J. Dudek, R. G. Edwards, and C. E. Thomas, Phys. Rev. D92 (2015) [Wilson15]

[2] J. J. Dudek et al. Phys. Rev. D87 (2013) [Dudek13]

[3] J. Bulava, B. Fahy, B. Hörz, K. J. Juge, C. Morningstar and C. H. Wong, Nucl. Phys. B910 (2016)

[4] J. Bulava, B. Hörz, B. Fahy, K. J. Juge, C. Morningstar and C. H. Wong, PoS LATTICE (2016)

[5] S. Aoki et al., Phys. Rev. D84 (2011)

[6] C. Alexandrou et al., Phys. Rev. D96 (2017)

[7] Z. Fu and L. Wang, Phys. Rev. D94 (2016)

$N_f = 2 + 1$ lattice data analysis

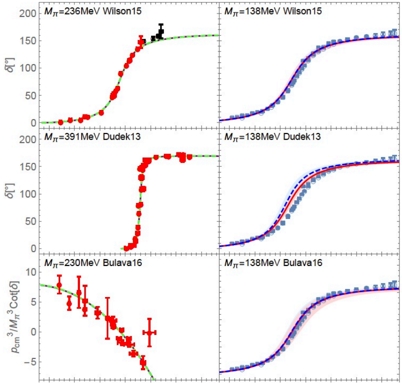

Figure: Left: Lattice data included in the fit are marked in red [Wilson15], [Dudek13], [Bulava16]. Right: Extrapolation to the physical point in comparison to the experimental data.

$N_f = 2 + 1$ lattice data analysis

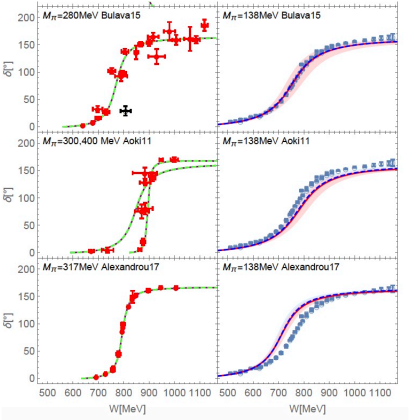

Figure: Left: Lattice data included in the fit are marked in red [Bulava15], [Aoki11] and [Alexandru17]. Right: Extrapolation to the physical point in comparison to the experimental data.

$N_f = 2 + 1$ lattice data analysis

	m_π [MeV]	$\hat{l}_1 \times 10^{-3}$	$\hat{l}_2 \times 10^{-3}$	$\chi^2_{d.o.f}$
Wilson15	236	3.7 ± 1.2	-3.2 ± 0.3	0.9
Dudek13	391	1.8 ± 0.5	-3.7 ± 0.3	1.2
Bulava16	230	5 ± 2	-3.1 ± 0.4	1.1
Aoki11	300& 400	2.5 ± 0.7	-2.8 ± 0.3	1.1
Alexandrou17	317	2.8 ± 0.8	-3.8 ± 0.3	0.6
HadSpec	236&391	2.0 ± 0.2	-3.6 ± 0.1	1.1
Guo16 ($N_f = 2$)	226&315	2.26 ± 0.14	-3.44 ± 0.03	1.3

Table: Low-energy constants and $\chi^2_{\rm d.o.f}$ obtained in the minimization for fixed $L_3 = -3.01 \times 10^{-3}$ and $L_5 = 0.64 \times 10^{-3}$.

$N_f = 2 + 1$ lattice data analysis

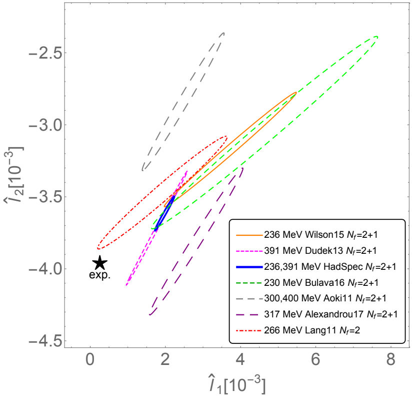

Figure: Error ellipses (68% confidence) in the minimization for the SU(3) analyses of the $N_f = 2 + 1$ lattice data sets. The red dash-dotted ellipse (Lang11) represents the uncertainties from the analysis of the $N_f = 2$ data using a one-channel SU(3) UChPT model

$N_f = 2+1$ lattice data analysis

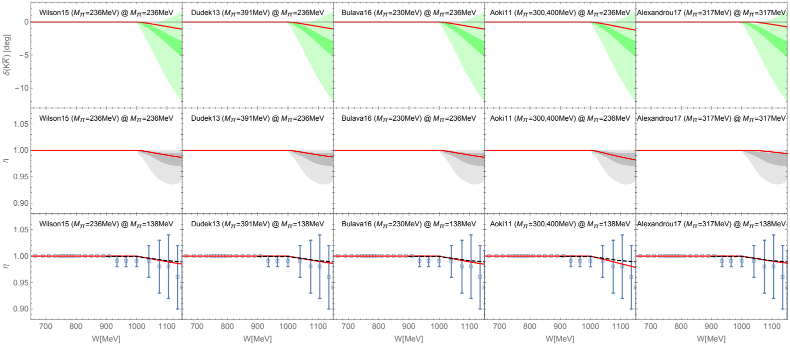

Figure: $K\bar{K}$ phase shifts (first row) and inelasticities (second row) obtained in the minimization for the different lattice data sets extrapolated at $m_\pi = 236$ MeV, in comparison with the result from [Wilson15] (bands). In the bottom row, the extrapolated inelasticity to the physical point, in comparison with the experimental data (squared), and with the Roy-Steiner solution (black-dashed lines).

$N_f = 2 + 1$ lattice data analysis

Combined fit of the Hadron Spectrum Col. data $m_\pi = 236, 391$ MeV

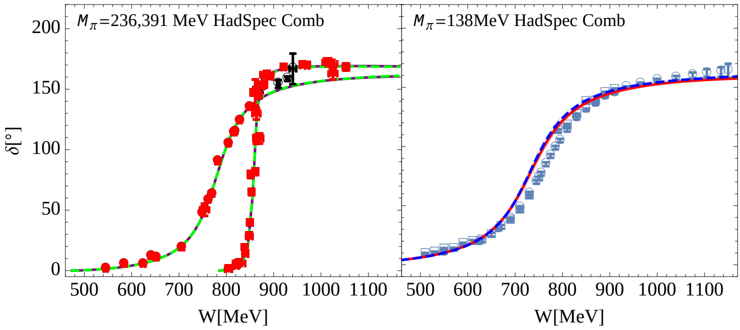

Figure: Left: Lattice data fitted (red). Right: Extrapolation to the physical point in comparison to the experimental data

Pion mass dependence of the ρ meson mass

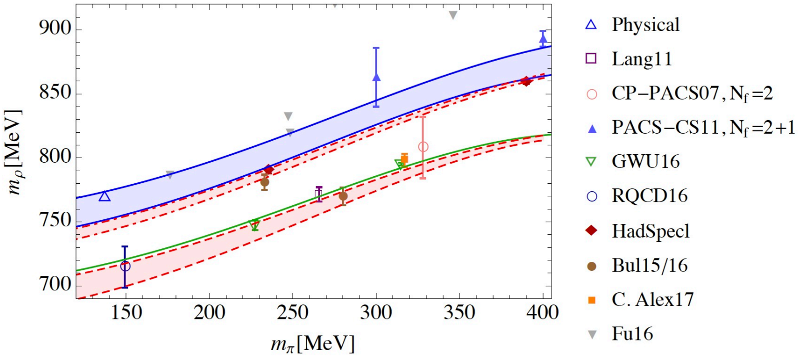

Figure: Pion mass dependence of the ρ meson mass. In red, the prediction from the combined fit of the HadSpec Collaboration in comparison with the SU(2) result

$N_f = 2 + 1$ lattice data analysis

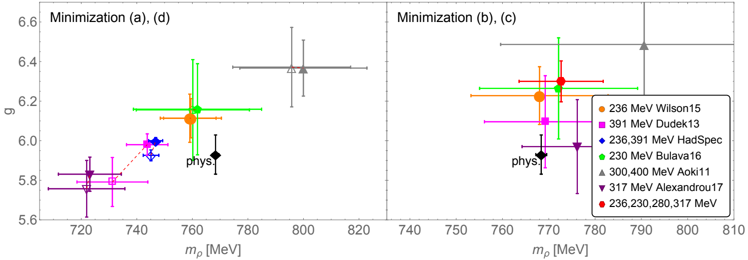

Figure: Coupling vs. the ρ mass in different minimizations.

Conclusions

- Unitarized Chiral Perturbation Theory is a powerful and simple model to study the pion mass dependence, which can be implemented in the finite volume to fit the energy levels.
- It different channels and partial waves and can be applied to sudy, the σ, ρ, K^*, κ,... and other resonances below 1.2 GeV
- Input from lattice: Energy levels or phase shifts, covariance matrix, decay constants (if possible)